Collision-Induced Absorption (CIA) cross-sections in HITRAN

Contacts: Iouli Gordon : `igordon@cfa.harvard.edu`*; Jacopo Terragni :* `jacopo.terragni@nasa.gov`

Collision-Induced Absorption (CIA) of infrared radiation contributes appreciably to the total absorption of radiation in planetary atmospheres. This section of the database has undergone a substantial update and extension for HITRAN2024. This extension is documented in detail in **Terragni *et al.* [A 1]**.

As in the original effort described in Richard *et al.* [A2], and subsequent update of Karman *et al.* [A3], only binary collisions are considered for inclusion. We continue to provide *Main* and *Alternate* folders to distinguish between data sets.

- The *Main* folder contains recommended sets of collision-induced absorptions.
- The *Alternate* folder contains two types of supplementary data:
  - The first type of data is simply alternative to that in the *Main* folder, in particular where the CIA parameterization is intended to be used in conjunction with a specific line-by-line list. Such as is the case for O_2-Air absorption in particular.
  - A second type of data in the *Alternate* folder is provided when the data are not generally recommended due to large uncertainties, and should therefore be used with caution. However, these data could have a clear advantage over the recommended set for specific applications, *e.g.* extended temperature ranges or to account for spin statistics.

Instructions for accessing the database can be found on the HITRAN website (`www.hitran.org/cia`). Figure 1 below illustrates the format of the headers for each individual data set. Table 1 provides a comprehensive summary of the CIA data that are presently available for HITRAN2024.

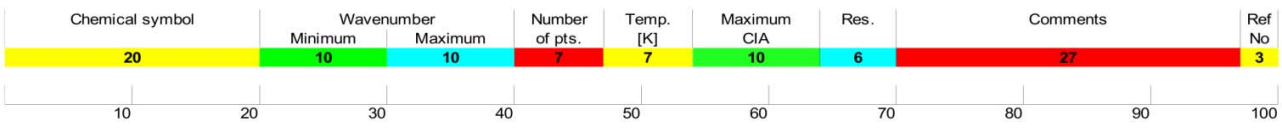

Figure 1: Definition of the HITRAN CIA header. The numbers indicate the length of each block. Reference numbers identify the sources of the data and are tabulated in Table 1.

Table 1: Summary of the different bands for all collisional pairs available in the HITRAN CIA database, both *Main* and *Alternate* folders. The band description specifies which (forbidden) monomer transitions the data set corresponds to and, where ambiguous, of which monomer. Note, the reference numbers in this table coincide with a CIA reference codes provided within the header of each CIA file and are ordered by collisional system.

System	Folder	ν range (cm^{-1})	T range (K)	# of sets	Band description	Reference
CH_4-Ar	Alternate	1-697	70-296	5	Roto-translational	[21]
CH_4-CH_4	Alternate	0-990	40-400	10	Roto-translational	[19]
CH_4-He	Main	1-1000	40-350	10	Roto-translational	[25]
CO_2-Ar	Main	0-300	200-400	21	Roto-translational	[41]
CO_2-CH_4	Main	0-720	100-600	6[a]	Roto-translational	[47]
	Alternate	0-2000	200-350	4[a]	Roto-translational	[28]
	Alternate	5-1200	100-600	6[a]	Roto-translational	[46]
CO_2-CO_2	Main	1-750	200-800	10	Roto-translational	[20]
	Main	1120-1800	375-500	6[a]	Fermi dyad	[57]
	Main	1150-1850	192-360	12[a]	Fermi dyad	[23]
	Main	2510-2850	221-297	3	Fermi triad	[38]
	Main	2850-3250	230-298	4[a]	$\nu_2 + \nu_3$ band	[49, 39]
	Main	4000-4500	260-295	2[a]	$3(\nu_1/2\nu_2)$ band	[49]
	Alternate	0-250	200-800	7	Roto-translational	[20]
CO_2-H_2	Main	5-1500	100-600	6[a]	Roto-translational	[46]
	Alternate	0-2000	200-350	4[a]	Roto-translational	[28]
CO_2-H_2O	Main	5700-6300	296	1[a]	$\nu_3(CO_2) + \nu_1(H_2O)$	[48]
CO_2-He	Main	0-1000	300	1	Roto-translational	[26]
H_2-CH_4	Main	0-1946	40-400	20[b]	Roto-translational	[16]
H_2-H	Main	100-10,000	1000-2500	4	Roto-translational, fundamental, 1^{st} overtone	[17]
H_2-H_2	Main	20-10,000	200-3000	113	Roto-translational, fundamental, 1^{st} overtone	[6]
	Alternate	0-2400	40-400	120[b,c]	Roto-translational	[34]
	Alternate	2500-6000	120-501	7[a]	Fundamental	[44]
	Alternate	7974-8650	293	1[a]	1^{st} overtone	[45]
H_2-He	Main	20-20,000	200-9900	334	Roto-translational, fundamental, 1^{st}-4^{th} overtone	[7]
	Alternate	0-2400	40-400	20[b]	Roto-translational	[14]
	Alternate	2500-6000	121-504	7[a]	H_2 fundamental	[44]
He-H	Main	50-11,000	1500-10,000	10	Roto-translational	[18]
N_2-Air	Main	1850-3000	301-363	5	N_2 fundamental	[2, 33]

Continued on next page

Table 1 – *Continued from previous page*

System	Folder	ν range (cm^{-1})	T range (K)	# of sets	Band description	Reference
	Main	2000-2698	228-272	5	N_2 fundamental	[3, 33]
	Main	4300-5000	200-330	14	N_2 1^{st} overtone	[24]
N_2-Ar	Main	0-300	70-500	44[a]	Roto-translational	[51]
	Main	2100-2600	300	1[a]	N_2 fundamental	[51]
	Alternate	2131-2559	300	1[a]	N_2 fundamental	[52]
N_2-CH_4	Main	0-800	70-400	34[a]	Roto-translational	[55]
	Alternate	0-1379	40-400	10	Roto-translational	[13]
N_2-H_2	Main	0-1886	40-400	10	Roto-translational	[12]
	Main	3900-5100	296	1[a]	H_2 fundamental	[50]
N_2-H_2O	Main	1930-2830	250-350	11	N_2 fundamental	[35]
N_2-He	Main	1-1000	300	1	Roto-translational	[26]
N_2-N_2	Main	0-450	70-200	14	Roto-translational	[40]
	Main	0-550	210-300	10	Roto-translational	[40]
	Main	0-650	310-400	10	Roto-translational	[40]
	Main	1850-3000	301-363	5	Fundamental	[2]
	Main	2000-2698	228-272	5	Fundamental	[3]
	Main	4300-5000	200-330	14	1^{st} overtone	[24]
	Alternate	30-300	78-129	4	Roto-translational	[36]
O_2-Air	Main	1300-1850	193-356	7	O_2 fundamental	[42, 43]
	Main	7545-8355	246-346	11[a]	$a^1\Delta_g \leftarrow X^3\Sigma_g^-(0,0)$	[53]
	Main	7583-8355	206-236	4[a]	$a^1\Delta_g \leftarrow X^3\Sigma_g^-(0,0)$	[58]
	Main	9091-9596	293	1	$a^1\Delta_g \leftarrow X^3\Sigma_g^-(1,0)$	[27]
	Main	10,512-11,228	293	1	$a^1\Delta_g \leftarrow X^3\Sigma_g^-(2,0)$	[29]
	Main	12,600-13,839	300	1	$b^1\Delta_g^+ \leftarrow X^3\Sigma_g^-(0,0)$	[4]
	Alternate	7583-8183	206-346	15	$a^1\Delta_g \leftarrow X^3\Sigma_g^-(0,0)$	[27]
	Alternate	9060-9960	206-346	15	$a^1\Delta_g \leftarrow X^3\Sigma_g^-(1,0)$	[27]
	Alternate	10,525-11,125	206-346	15	$a^1\Delta_g \leftarrow X^3\Sigma_g^-(2,0)$	[27]
	Alternate	12,804-13,402	206-346	15	$b^1\Delta_g^+ \leftarrow X^3\Sigma_g^-(0,0)$	[27]
	Alternate	12,990-13,220	298	1	$b^1\Delta_g^+ \leftarrow X^3\Sigma_g^-(0,0)$	[22]
	Alternate	14,296-14,806	206-346	15	$b^1\Delta_g^+ \leftarrow X^3\Sigma_g^-(1,0)$	[27]
O_2-CO_2	Main	9105-9545	293	1[a]	$a^1\Delta_g \leftarrow X^3\Sigma_g^-(1,0)$	[56]
	Main	12,600-13,839	296	1	$b^1\Delta_g^+ \leftarrow X^3\Sigma_g^-(0,0)$	[5]
O_2-N_2	Main	1300-1850	193-356	7	O_2 fundamental	[42, 43]
	Main	1850-3000	301-363	5	N_2 fundamental	[2, 33]
	Main	2000-2698	228-272	5	N_2 fundamental	[3, 33]
	Main	7545-8355	246-346	11[a]	$a^1\Delta_g \leftarrow X^3\Sigma_g^-(0,0)$	[53]
	Main	7583-8355	206-236	4[a]	$a^1\Delta_g \leftarrow X^3\Sigma_g^-(0,0)$	[58]
	Main	12,600-13,840	296	1	$b^1\Delta_g \leftarrow X^3\Sigma_g^-(0,0)$	[4]

Continued on next page

Table 1 – *Continued from previous page*

System	Folder	ν range (cm^{-1})	T range (K)	# of sets	Band description	Reference
	Alternate	7583-8133	206-346	15	$a^1\Delta_g \leftarrow X^3\Sigma_g^-(0,0)$	[27]
	Alternate	12,804-13,402	206-346	15	$b^1\Delta_g \leftarrow X^3\Sigma_g^-(0,0)$	[27]
O_2-O_2	Main	1150-1950	193-353	15	Fundamental	[2]
	Main	7545-8355	246-346	11[a]	$a^1\Delta_g \leftarrow X^3\Sigma_g^-(0,0)$	[53]
	Main	7583-8355	206-236	4[a]	$a^1\Delta_g \leftarrow X^3\Sigma_g^-(0,0)$	[58]
	Main	9060-9596	293	1	$a^1\Delta_g \leftarrow X^3\Sigma_g^-(1,0)$	[27]
	Main	10,512-11,228	293	1	$a^1\Delta_g \leftarrow X^3\Sigma_g^-(2,0)$	[29]
	Main	12,600-13,839	296	1	$b^1\Sigma_g^+ \leftarrow X^3\Sigma_g^-(0,0)$	[4]
	Main	14,206-14,898	293	1	$b^1\Sigma_g^+ \leftarrow X^3\Sigma_g^-(1,0)$	[30]
	Main	15,290-16,664	203-287	4	Double transitions*	[32]
	Main	16,644-19,628	203-293	5	Double transitions*	[32]
	Main	20,000-33,670	223-293	3[a]	Double transitions*	[54]
	Alternate	1300-1850	193-356	7	Fundamental	[42, 43]
	Alternate	7583-8183	206-346	15	$a^1\Delta_g \leftarrow X^3\Sigma_g^-(0,0)$	[27]
	Alternate	9060-9960	206-346	15	$a^1\Delta_g \leftarrow X^3\Sigma_g^-(1,0)$	[27]
	Alternate	10,535-11,125	206-346	15	$a^1\Delta_g \leftarrow X^3\Sigma_g^-(2,0)$	[27]
	Alternate	12,804-13,402	206-346	15	$b^1\Delta_g^+ \leftarrow X^3\Sigma_g^-(0,0)$	[27]
	Alternate	14,296-14,806	206-346	15	$b^1\Delta_g^+ \leftarrow X^3\Sigma_g^-(1,0)$	[27]

[a] CIA sets are newly added, updated, or have changed folder for HITRAN2024

[b] 10 data sets are provided for "equilibrium" H_2 and 10 data sets are also provided for "normal" H_2, which has a 3:1 ortho:para ratio

[c] In addition, 10 conditions for out-of-equilibrium H_2 ortho:para ratios are provided, with 10 data sets per ratio

General definitions

The attenuation of light by a gas with absorption coefficient $k(\nu)$ is given by the Lambert law

$$-\ln\left[T\left(\nu\right)\right] = k(\nu)L, \tag{1}$$

where $T(\nu)$ is the transmittance at wave number ν, and L is the optical path length. Leaving aside pressure variations in the line shape of resonant transitions of an individual molecule, the absorption coefficient is given by the virial expansion in the number density ρ

$$k(\nu) = k^{(1)}(\nu)\ \rho + k^{(2)}(\nu)\ \rho^2 + \ldots, \tag{2}$$

which permits discrimination of monomer absorption and absorption by molecular pairs or ternary and larger complexes of colliding molecules. The absorption by collision complexes involving more than two molecules is expected to be insignificant under typical atmospheric conditions, even for planets with dense atmospheres such as Venus, and is thus disregarded here.

In HITRAN units, the density ρ is given in molecule cm^{-3}. The monomer absorption cross section $k^{(1)}(\nu)$ is given in cm^2 molecule^{-1}, and is tabulated in HITRAN for many molecules relevant to planetary atmospheres. The contribution of binary complexes is given by the CIA absorption coefficient, $k^{(2)}(\nu)$, which is tabulated in the HITRAN CIA section discussed in this paper, in units of cm^5 molecule^{-2}. The frequency and absorption coefficient are tabulated in two-column format, where each band and temperature set is preceded by a header, formatted as defined in Figure 1.

For mixtures containing multiple molecular species, for example A and B, the binary contributions take the form

$$k(\nu) = k^{(A-A)}(\nu)\ \rho_A^2 + k^{(A-B)}(\nu)\ \rho_A\rho_B + k^{(B-B)}(\nu)\ \rho_B^2, \tag{3}$$

where ρ_A and ρ_B are the number densities of both molecular species. The current updated version of the HITRAN CIA database consistently tabulates binary CIA absorption coefficients $k^{(A-A)}(\nu)$, $k^{(A-B)}(\nu)$, and $k^{(B-B)}(\nu)$, separately. By contrast, the previous version of the database also listed coefficients for different mixtures which had to be scaled with the square of the *total* number density $(\rho_A + \rho_B)^2$. This may have been confusing, and lead to deviations from Eq. (3)–especially when combined with interpolation or extrapolation schemes–and it was inconsistent with the tabulation of theoretical results which obtain $k^{(A-A)}(\nu)$, $k^{(A-B)}(\nu)$, or $k^{(B-B)}(\nu)$ directly, without using mixtures. Fortunately, the only system for which results with different mixtures were previously reported was $O_2 - N_2$. This issue has been fixed in the HITRAN 2016 update [A4].

Also introduced in the HITRAN 2016 update was the concept of an $M -$ Air CIA section, which aims to combine $M - O_2$, $M - N_2$, and $M -$ Ar as ready-to-use absorption

coefficients for applications for the Earth's atmosphere. To be explicit,

$$-\frac{\ln\left[T(\nu)\right]}{L} = k^{(M-\mathrm{Air})}(\nu)\ \rho_M \rho_{\mathrm{Air}}, \tag{4}$$

with $\rho_{\mathrm{Air}} = \rho_{\mathrm{O_2}} + \rho_{\mathrm{N_2}}$. The $M-$Air data typically come from three sources:

1. The data may contain the sum of $M-\mathrm{O_2}$, $M-\mathrm{N_2}$, and $M-$Ar contributions, where these are separately available. These data should be consistent and hence preferably from the same source, which may be either experimental or obtained from calculations.

2. In many cases the 1% $M-$Ar data will be unavailable. In these cases, we typically provide 21:79 or 22:78 mixtures of $M-\mathrm{O_2}$:$M-\mathrm{N_2}$ contributions, depending on whether $\mathrm{O_2}$ or $\mathrm{N_2}$ is to be considered the better model for Ar, which may depend on the transition considered.

3. The data provided as $M-$Air may also directly come from experiments using either air or a similar mixture, e.g. synthetic air.

In summary: where available, the $M-$Air CIA section gives the recommended binary absorption coefficient. Users should not double count contributions by explicitly adding the contributions of $M-\mathrm{O_2}$, $M-\mathrm{N_2}$ or $M-$Ar, which are already accounted for.

Unlike the *line-by-line* and *cross-sections* parts of the HITRAN database which are cast into the SQL structure described in Hill *et al.* [A5], the CIA files are still provided in static ASCII format accompanied with a reference Table (`https://hitran.org/data/CIA/Collision-Induced-Absorption_references_2024.pdf`), which is consistent with the referencing in this Readme. In the near future, CIA parameters will also be cast into SQL structure. Access through the HITRAN Application Programming Interface (HAPI) [A6] will also be enabled. Thus, calculations of absorption coefficients, cross-sections, etc using HAPI will be implemented.

Acknowledgments

This document was prepared with contributions from I. E. Gordon, J. Terragni, T. Karman, R. J. Hargreaves, C. Richard, A. A. Finenko, and L. S. Rothman.

Collision Induced Absorption (CIA) reference numbers

The following reference numbers can be found in the data headers of the HITRAN CIA files and coincide with the reference numbers in Table 1.

[1] K. M. Smith, D. A. Newnham, Near-infrared absorption cross sections and integrated absorption intensities of molecular oxygen (O_2, O_2-O_2, and O_2-N_2), Journal of Geophysical Research Atmospheres 105 (D6) (2000) 7383–7396. doi:10.1029/1999JD901171.

[2] Y. Baranov, W. Lafferty, G. Fraser, Investigation of collision-induced absorption in the vibrational fundamental bands of O_2 and N_2 at elevated temperatures, J. Mol. Spectrosc. 233 (1) (2005) 160 – 163. doi:10.1016/j.jms.2005.06.008.

[3] W. J. Lafferty, A. M. Solodov, A. Weber, W. B. Olson, J.-M. Hartmann, Infrared collision-induced absorption by N_2 near 4.3 μm for atmospheric applications: measurements and empirical modeling, Applied Optics 35 (30) (1996) 5911. doi:10.1364/AO.35.005911.

[4] H. Tran, C. Boulet, J.-M. Hartmann, Line mixing and collision-induced absorption by oxygen in the A-band: Laboratory measurements, model, and tools for atmospheric spectra computations, J. Geophys. Res. 111 (2006) D15210. doi:10.1029/2005JD006869.

[5] M. Vangvichith, H. Tran, J.-M. Hartmann, Line-mixing and collision induced absorption for O_2–CO_2 mixtures in the oxygen A-band region, J. Quant. Spectrosc. Radiat. Transfer 110 (18) (2009) 2212–2216. doi:10.1016/j.jqsrt.2009.06.002.

[6] M. Abel, L. Frommhold, X. Li, K. L. C. Hunt, Collision-induced absorption by H_2 pairs: From hundreds to thousands of Kelvin, J. Phys. Chem. A 115 (25) (2011) 6805–6812. doi:10.1021/jp109441f.

[7] M. Abel, L. Frommhold, X. Li, K. L. C. Hunt, Infrared absorption by collisional H_2–He complexes at temperatures up to 9000 K and frequencies from 0 to 20000 cm^1, J. Chem. Phys. 136 (4) (2012) 044319. doi:10.1063/1.3676405.

[8] G. D. Greenblatt, J. J. Orlando, J. B. Burkhoder, A. R. Ravishankara, Absorption measurements of oxygen between 330 and 1140 nm, J. Geophys. Res. 95 (1990) 18577. doi:10.1029/JD095iD11p18577.

[9] C. Hermans, Measurement of absorption cross sections and spectroscopic molecular parameters, http://spectrolab.aeronomie.be/o2.htm.

[10] Maté, B. and Lugez, C. and Fraser, G. T. and Lafferty, W. J., Absolute intensities for the O_2 1.27 μm continuum absorption, J. Geophys. Res.: Atmospheres 104 (D23) (1999) 30585–30590. doi:10.1029/1999JD900824.

[11] A. Borysow, L. Frommhold, Collision-induced rototranslational absorption spectra of N_2-N_2 pairs for temperatures from 50 to 300 K, Astrophys. J. 311 (1986) 1043–1057. doi:10.1086/164841.

[12] A. Borysow, L. Frommhold, Theoretical Collision-induced Rototranslational Absorption Spectra for Modeling Titan's Atmosphere: H_2–N_2 Pairs, Astrophysical Journal 303 (1986) 495. doi:10.1086/164096.

[13] A. Borysow, C. Tang, Far Infrared CIA Spectra of N_2-CH_4 Pairs for Modeling of Titan's Atmosphere, Icarus 105 (1) (1993) 175–183. doi:10.1006/icar.1993.1117.

[14] J. Borysow, L. Frommhold, G. Birnbaum, Collision-induced Rototranslational Absorption Spectra of H_2-He Pairs at Temperatures from 40 to 3000 K, Astrophysical Journal 326 (1988) 509. doi:10.1086/166112.

[15] G. S. Orton, M. Gustafsson, M. Burgdorf, V. Meadows, Revised *ab initio* models for H_2-H_2 collision-induced absorption at low temperatures, Icarus 189 (2) (2007) 544–549. doi:10.1016/j.icarus.2007.02.003.

[16] A. Borysow, L. Frommhold, Theoretical Collision-induced Rototranslational Absorption Spectra for the Outer Planets: H_2–CH_4 Pairs, Astrophysical Journal 304 (1986) 849. doi:10.1086/164221.

[17] M. Gustafsson, L. Frommhold, The H_2–H infrared absorption bands at temperatures from 1000 K to 2500 K, Astronomy & Astrophysics 400 (3) (2003) 1161–1162. doi:10.1051/0004-6361:20030100.

[18] M. Gustafsson, L. Frommhold, Infrared Absorption Spectra of Collisionally Interacting He and H Atoms, Astrophysical Journal 546 (2) (2001) 1168–1170. doi:10.1086/318311.

[19] A. Borysow, L. Frommhold, Collision-induced Rototranslational Absorption Spectra of CH_4-CH_4 Pairs at Temperatures from 50 to 300 K, Astrophysical Journal 318 (1987) 940. doi:10.1086/165426.

[20] M. Gruszka, A. Borysow, Roto-translational collision-induced absorption of CO_2 for the atmosphere of Venus at frequencies from 0 to 250 cm^{-1}, at temperatures from 200 to 800 K, Icarus 129 (1997) 172. doi:10.1006/icar.1997.5773.

[21] R. E. Samuelson, N. R. Nath, A. Borysow, Gaseous abundances and methane supersaturation in Titan's troposphere, Planetary and Space Science 45 (8) (1997) 959–980. doi:10.1016/S0032-0633(97)00090-1.

[22] B. J. Drouin, D. C. Benner, L. R. Brown, M. J. Cich, T. J. Crawford, V. M. Devi, A. Guillaume, J. T. Hodges, E. J. Mlawer, D. J. Robichaud, F. Oyafuso, V. H. Payne, K. Sung, E. H. Wishnow, S. Yu, Multispectrum analysis of the oxygen

A-band, J. Quant. Spectrosc. Radiat. Transfer 186 (2017) 118. doi:10.1016/j.jqsrt.2016.03.037.

[23] Y. I. Baranov, W. J. Lafferty, G. T. Fraser, Infrared spectrum of the continuum and dimer absorption in the vicinity of the O_2 vibrational fundamental in O_2/CO_2 mixtures, Journal of Molecular Spectroscopy 228 (2) (2004) 432–440. doi:10.1016/j.jms.2004.04.010.

[24] J.-M. Hartmann, C. Boulet, G. C. Toon, Collision-induced absorption by N_2 near 2.16 μm: Calculations, model, and consequences for atmospheric remote sensing, J. Geophys. Res.: Atmos. 122 (2017) 2419. doi:10.1002/2016JD025677.

[25] R. H. Taylor, A. Borysow, L. Frommhold, Concerning the rototranslational absorption spectra of He–CH_4 pairs, J. Mol. Spectrosc. 129 (1988) 45. doi:10.1016/0022-2852(88)90257-3.

[26] E. Bar-Ziv, S. Weiss, Translational Spectra Due to Collision-Induced Overlap Moments in Mixtures of He with CO_2, N_2, CH_4, and C_2H_6, J. Chem. Phys. 57 (1972) 34. doi:10.1063/1.1677970.

[27] T. Karman, M. A. J. Koenis, A. Banerjee, D. H. Parker, I. E. Gordon, A. van der Avoird, W. J. van der Zande, G. C. Groenenboom, O_2-O_2 and O_2-N_2 collision-induced absorption mechanisms unravelled, Nature Chem. 10 (2018) 549. doi:10.1038/s41557-018-0015-x.

[28] R. Wordsworth, Y. Kalugina, S. Lokshtanov, A. Vigasin, B. Ehlmann, J. Head, C. Sanders, H. Wang, Transient reducing greenhouse warming on early Mars, Geophys. Res. Lett. 44 (2017) 665. doi:10.1002/2016GL071766.

[29] F. R. Spiering, W. J. van der Zande, Collision induced absorption in the $a^1\Delta(\nu{=}2) \leftarrow X^3\Sigma_g^-(\nu{=}0)$ band of molecular oxygen, Phys. Chem. Chem. Phys. 14 (28) (2012) 9923–9928. doi:10.1039/c2cp40961e.

[30] F. R. Spiering, M. B. Kiseleva, N. N. Filippov, L. van Kesteren, W. J. van der Zande, Collision-induced absorption in the O_2 B-band region near 670 nm, Phys. Chem. Chem. Phys. 13 (2011) 9616–9621. doi:10.1039/C1CP20403C.

[31] T. Karman, E. Miliordos, K. L. C. Hunt, G. C. Groenenboom, A. van der Avoird, Quantum mechanical calculation of the collision-induced absorption spectra of N_2–N_2 with anisotropic interactions, J. Chem. Phys. 142 (2015) 084306. doi:10.1063/1.4907917.

[32] R. Thalman, R. Volkamer, Temperature dependent absorption cross-sections of O_2-O_2 collision pairs between 340 and 630 nm and at atmospherically relevant pressure, Phys. Chem. Chem. Phys. 15 (37) (2013) 15371. doi:10.1039/c3cp50968k.

[33] Estimated from N_2-N_2 data from Refs. [2, 3] using Eq. (7) of Ref. [3], which is derived using data from the following paper:
• V. Menoux, R. L. Doucen, C. Boulet, A. Roblin, A. M. Bouchardy, Collision-induced absorption in the fundamental band of N_2: Temperature dependence of the absorption for N_2-N_2 and N_2-O_2 pairs., Applied optics 32 (3) (1993) 263–268. doi:10.1364/AO.32.000263.

[34] L. N. Fletcher, M. Gustafsson, G. S. Orton, Hydrogen Dimers in Giant-planet Infrared Spectra, Astrophysical Journal Supplement Series 235 (1) (2018) 24. doi:10.3847/1538-4365/aaa07a.

[35] J.-M. Hartmann, C. Boulet, D. D. Tran, H. Tran, Y. Baranov, Effect of humidity on the absorption continua of CO_2 and N_2 near 4 μm: Calculations, comparisons with measurements, and consequences for atmospheric spectra, Journal of Chemical Physics 148 (5) (2018) 054304. doi:10.1063/1.5019994.

[36] E. Wishnow, K. Sung, et al., The far-infrared collision-induced spectrum of nitrogen over the temperature range 78–129 K, J. Quant. Spectrosc. Radiat. Transfer, in preparation (2018).

[37] Y. Baranov, A. Vigasin, Collision-induced absorption by CO_2 in the region of ν_1, $2\nu_2$, J. Mol. Spectrosc. 193 (2) (1999) 319 – 325. doi:10.1006/jmsp.1998.7743.

[38] Y. Baranov, G. T. Fraser, W. J. Lafferty, A. Vigasin, Collision-induced absorption in the CO_2 fermi triad for temperatures from 211 K to 296 K, in: C. Camy-Peyret, A. Vigasin (Eds.), Weakly Interacting Molecular Pairs: Unconventional Absorbers of Radiation in the Atmosphere, Springer, 2003, pp. 149–158. doi:10.1007/978-94-010-0025-3_12.

[39] Y. I. Baranov, Collision-induced absorption in the region of the $\nu_2+\nu_3$ band of carbon dioxide, J. Mol. Spectrosc. 345 (2018) 11 – 16. doi:10.1016/j.jms.2017.11.005.

[40] D. N. Chistikov, A. A. Finenko, S. E. Lokshtanov, S. V. Petrov, A. A. Vigasin, Simulation of collision-induced absorption spectra based on classical trajectories and ab initio potential and induced dipole surfaces. I. Case study of N_2-N_2 rototranslational band, Journal of Chemical Physics 151 (19). doi:10.1063/1.5125756.

[41] T. Odintsova, E. Serov, A. Balashov, M. Koshelev, A. Koroleva, A. Simonova, M. Tretyakov, N. Filippov, D. Chistikov, A. Finenko, S. Lokshtanov, S. Petrov, A. Vigasin, CO_2-CO_2 and CO_2-Ar continua at millimeter wavelengths, Journal of Quantitative Spectroscopy and Radiative Transfer 258. doi:10.1016/j.jqsrt.2020.107400.

[42] F. Thibault, V. Menoux, R. Le Doucen, L. Rosenmann, J.-M. Hartmann, C. Boulet, Infrared collision-induced absorption by O_2 near 6.4 μm for atmospheric

applications: measurements and empirical modeling, Applied Optics 36 (3) (1997) 563. doi:10.1364/ao.36.000563.

[43] J. J. Orlando, G. S. Tyndall, K. E. Nickerson, J. G. Calvert, The temperature dependence of collision-induced absorption by oxygen near 6 μm, Journal of Geophysical Research: Atmospheres 96 (D11) (1991) 20 755–20 760. doi:10.1029/91JD02042.

[44] F. Vitali, S. Stefani, G. Piccioni, M. Snels, D. Grassi, D. Biondi, A. Boccaccini, New experimental measurements of the Collision Induced Absorptions of H_2-H_2 and H_2-He in the 3600-5500 cm^{-1} spectral range from 120 to 500 K, Journal of Quantitative Spectroscopy and Radiative Transfer 330 (2025) 109255. doi:10.1016/j.jqsrt.2024.109255.

[45] A. O. Koroleva, S. Kassi, H. Fleurbaey, A. Campargue, The collision-induced absorption of H_2 near 1.20 μm: Subatmospheric measurements and validation tests of calculations, Journal of Quantitative Spectroscopy and Radiative Transfer 318 (2024) 108948. doi:10.1016/j.jqsrt.2024.108948.

[46] M. Turbet, C. Boulet, T. Karman, Measurements and semi-empirical calculations of CO_2+CH_4 and CO_2+H_2 collision-induced absorption across a wide range of wavelengths and temperatures. Application for the prediction of early Mars surface temperature, Icarus 346 (2020) 113762. doi:10.1016/j.icarus.2020.113762.

[47] W. Fakhardji, C. Boulet, H. Tran, J.-M. Hartmann, Direct calculations of the CH_4+CO_2 far infrared collision-induced absorption, Journal of Quantitative Spectroscopy and Radiative Transfer 283 (2022) 108148. doi:10.1016/j.jqsrt.2022.108148.

[48] H. Fleurbaey, D. Mondelain, W. Fakhardji, J. M. Hartmann, A. Campargue, Simultaneous collision-induced transitions in H_2O+CO_2 gas mixtures, Journal of Quantitative Spectroscopy and Radiative Transfer 285 (2022) 108162. doi:10.1016/j.jqsrt.2022.108162.

[49] H. Tran, J. M. Hartmann, E. Rambinison, M. Turbet, Collision-induced absorptions by pure CO_2 in the infrared: New measurements in the 1150–4500 cm^{-1} spectral range and empirical modeling for applications, Icarus 422 (2024) 116265. doi:10.1016/j.icarus.2024.116265.

[50] C. Wei, A. Klingberg, C. L. Strand, R. K. Hanson, Measurement of hydrogen and nitrogen via collision-induced infrared absorption, International Journal of Hydrogen Energy 93 (2024) 364–373. doi:10.1016/j.ijhydene.2024.10.318.

[51] E. A. Serov, T. A. Galanina, A. O. Koroleva, D. S. Makarov, I. S. Amerkhanov, M. A. Koshelev, M. Y. Tretyakov, D. N. Chistikov, A. A. Finenko, A. A. Vigasin, Continuum absorption in pure N_2 gas and in its mixture with Ar, Jour-

nal of Quantitative Spectroscopy and Radiative Transfer 328 (2024) 109172. doi:10.1016/j.jqsrt.2024.109172.

[52] G. Moreau, Étude en temperature et modélisation de l'absorption induite par collision dans les régions des bandes fondamentales pour les mélanges des gaz N_2-Ar et O_2, Ph.D. thesis, Université de Rennes (1999).
URL https://theses.fr/1999REN10083

[53] Coefficients were derived from measurements carried out at 271, 297 and 332 K by cavity ring down spectroscopy and described in the following two papers:
• D. Mondelain, S. Kassi, A. Campargue, Accurate Laboratory Measurement of the O_2 Collision-Induced Absorption Band Near 1.27 μm, Journal of Geophysical Research (Atmospheres) 124 (1) (2019) 414423. doi:10.1029/2018JD029317
• S. Kassi, S. Guessoum, J. C. A. Abanto, H. Tran, A. Campargue, D. Mondelain, Temperature Dependence of the Collision-Induced Absorption Band of O_2 Near 1.27 μm, Journal of Geophysical Research (Atmospheres) 126 (13) (2021) e2021JD034860. doi:10.1029/2021JD034860 .

[54] H. Finkenzeller, R. Volkamer, O_2-O_2 CIA in the gas phase: Cross-section of weak bands, and continuum absorption between 297-500 nm, Journal of Quantitative Spectroscopy and Radiative Transfer 279 (2022) 108063. doi:10.1016/j.jqsrt.2021.108063.

[55] A. A. Finenko, B. Bézard, I. E. Gordon, D. N. Chistikov, S. E. Lokshtanov, S. V. Petrov, A. A. Vigasin, Trajectory-based Simulation of Far-infrared Collision-induced Absorption Profiles of CH_4-N_2 for Modeling Titan's Atmosphere, Astrophysical Journal Supplement Series 258 (2) (2022) 33. doi:10.3847/1538-4365/ac36d3.

[56] A. Banerjee, J. Mandon, F. Harren, D. H. Parker, Collision-induced absorption between O_2-CO_2 for the $a^1\Delta_g$ (v = 1) $\leftarrow$ $X^3\Sigma_{-g}$ (v = 0) transition of molecular oxygen at 1060 nm, Physical Chemistry Chemical Physics (Incorporating Faraday Transactions) 21 (4) (2019) 1805–1811. doi:10.1039/C8CP06778C.

[57] J. Terragni, E. Kohler, V. Kofman, S. Anderson, G. L. Villanueva, S. Faggi, New Measurements of High-Temperature CO_2-CO_2 Collision-Induced Absorption in the 1100-1800 cm^{-1} Range, Journal of Quantitative Spectroscopy and Radiative Transfer 346 (2025) 109595. doi:10.1016/j.jqsrt.2025.109595.

[58] E. M. Adkins, T. Karman, A. Campargue, D. Mondelain, J. T. Hodges, Parameterized model to approximate theoretical collision-induced absorption band shapes for O_2-O_2 and O_2-N_2, Journal of Quantitative Spectroscopy and Radiative Transfer 310 (2023) 108732. doi:10.1016/j.jqsrt.2023.108732.

Additional references in this Readme

[A1] J. Terragni, I. E. Gordon, E. M. Adkins, C. Boulet, A. Campargue, D. Chistikov, A. Finenko, H. Finkenzeller, H. Fleurbaey, R. J. Hargreaves, R. K. Hanson, J.-M. Hartmann, A. Klingberg, E. Kohler, A. O. Koroleva, D. Mondelain, G. Piccioni, S. Stefani, C. L. Strand, H. Tran, M. Turbet, A. Vigasin, F. Vitali, R. Volkamer, C. Wei, Collision Induced Absorption in HITRAN2024: Enhanced and Improved Data for Atmospheric and Planetary Studies, Journal of Quantitative Spectroscopy and Radiative Transfer (2025) 109631. doi:10.1016/j.jqsrt.2025.109631.

[A2] C. Richard, I. Gordon, L. Rothman, M. Abel, L. Frommhold, M. Gustafsson, J.-M. Hartmann, C. Hermans, W. Lafferty, G. Orton, K. Smith, H. Tran, New section of the HITRAN database: Collision-induced absorption (CIA), J. Quant. Spectrosc. Radiat. Transfer 113 (2012) 1276. doi:10.1016/j.jqsrt.2011.11.004.

[A3] T. Karman, I. E. Gordon, A. van der Avoird, Y. I. Baranov, C. Boulet, B. J. Drouin, G. C. Groenenboom, M. Gustafsson, J.-M. Hartmann, R. L. Kurucz, L. S. Rothman, K. Sun, K. Sung, R. Thalman, H. Tran, E. H. Wishnow, R. Wordsworth, A. A. Vigasin, R. Volkamer, W. J. van der Zande, Update of the HITRAN collision-induced absorption section, Icarus 328 (2019) 160–175. doi:10.1016/j.icarus.2019.02.034.

[A4] I. E. Gordon, L. Rothman, C. Hill, R. Kochanov, Y. Tan, P. Bernath, M. Birk, V. Boudon, A. Campargue, K. Chance, B. Drouin, J.-M. Flaud, R. Gamache, J. Hodges, D. Jacquemart, V. Perevalov, A. Perrin, K. Shine, M.-A. Smith, J. Tennyson, G. Toon, H. Tran, V. Tyuterev, A. Barbe, A. Császár, V. Devi, T. Furtenbacher, J. Harrison, J.-M. Hartmann, A. Jolly, T. Johnson, T. Karman, I. Kleiner, A. Kyuberis, J. Loos, O. Lyulin, S. Massie, S. Mikhailenko, N. Moazzen-Ahmadi, H. Müller, O. Naumenko, A. Nikitin, O. Polyansky, M. Rey, M. Rotger, S. Sharpe, K. Sung, E. Starikova, S. Tashkun, J. V. Auwera, G. Wagner, J. Wilzewski, P. Wcisło, S. Yu, E. Zak, The HITRAN2016 molecular spectroscopic database, J. Quant. Spectrosc. Radiat. Transfer 203 (2017) 3. doi:10.1016/j.jqsrt.2017.06.038.

[A5] C. Hill, I. E. Gordon, R. V. Kochanov, L. Barrett, J. S. Wilzewski, L. S. Rothman, HITRANonline: An online interface and the flexible representation of spectroscopic data in the HITRAN database, J. Quant. Spectrosc. Radiat. Transfer 177 (2016) 4–14. doi:10.1016/j.jqsrt.2015.12.012.

[A6] R. V. Kochanov, I. E. Gordon, L. S. Rothman, P. Wcisło, C. Hill, J. S. Wilzewski, HITRAN Application Programming Interface (HAPI): A comprehensive approach to working with spectroscopic data, J. Quant. Spectrosc. Radiat. Transfer 177 (2016) 15–30. doi:10.1016/j.jqsrt.2016.03.005.